Dalton Transactions

Amorphous Fe2+-rich FeOx loaded in mesoporous silica as a highly efficient heterogeneous Fenton catalyst

Journal:	*Dalton Transactions*
Manuscript ID:	DT-ART-01-2014-000105.R2
Article Type:	Paper
Date Submitted by the Author:	07-Mar-2014
Complete List of Authors:	Wang, Min; shanghai institute of ceramics, Shu, Zhu; Faculty of Material Science and Chemistry, China University of Geosciences, Zhang, Lingxia; shanghai institute of ceramics, Fan, Xiangqian; shanghai institute of ceramics, Tao, Guiju; shanghai institute of ceramics, Wang, Yongxia; shanghai institute of ceramics, Chen, Lisong; shanghai institute of ceramics, Wu, Meiying; shanghai institute of ceramics, Shi, Jianlin; shanghai institute of ceramics, ;

Dalton Transactions

Dalton Transactions

Dynamic Article Links ►

Cite this: DOI: 10.1039/c0xx00000x

www.rsc.org/xxxxxx

Paper

Amorphous Fe^{2+}-rich FeO_x loaded in mesoporous silica as a highly efficient heterogeneous Fenton catalyst

Min Wang[a], Zhu Shu[b], Lingxia Zhang*[a], Xiangqian Fan[a], Guiju Tao[a], Yongxia Wang[a], Lisong Chen[a], Meiying Wu[a], Jianlin Shi*[a]

Received (in XXX, XXX) Xth XXXXXXXXX 20XX, Accepted Xth XXXXXXXXX 20XX
DOI: 10.1039/b000000x

A simple physical-vapor-infiltration (PVI) method using ferrocene as iron source, has been developed to load FeO_x into pore channels of mesoporous silica SBA-15. The obtained FeO_x/SBA-15 composite has a high loading amount of FeO_x (e.g. 26.64 wt% Fe content obtained at PVI duration 17 h and calcination temperature 450 ºC) but unblocked pore channels thanks to the unique preparation strategy. The FeO_x species are amorphous, rich of Fe^{2+} and have been highly dispersed as a nanocoating onto the pore channel surface. The FeO_x/ SBA-15 were used as heterogeneous Fenton catalysts to degrade Acid orange 7 (AO7). They showed high catalytic activity and degradation efficiency, which was attributed to the high proportion of Fe^{2+} in amorphous FeO_x and their favorable adsorption capability for the dye. The influences of PVI duration, calcination temperature and Fenton reaction conditions (FeO_x/SBA-15 dosages, H_2O_2 dosages and initial pH value) on their catalytic activity were investigated in detail.

Introduction

Numerous dyes are being produced in various chemical industries, especially in textile industry, in large scale every day. The heavy emissions of dyeing wastewater cause serious water pollution and ecological deterioration. Even a very small amount of dyes of as low as 1 ppm in concentrations can result in distinct color change of water [1]. More terribly, these dyeing wastewaters are considered to be carcinogenic, mutagenic and toxic threats to human being and aquatic lives [2]. However, many biologically toxic molecules are rather environmentally stable and cannot be well-degraded by commonly used physical, chemical and biological methods for water treatments [3]. Advanced oxidation process (AOP) which relies on highly oxidizing HO• (oxidation potential E_0 = 2.80 V [4]) to non-selectively degrade these biologically toxic or non-degradable organic contaminants into CO_2 or biodegradable small organic molecules [5] is the most promising strategy for wastewater treatment.

Fenton reaction, based on H_2O_2 and Fe^{2+}, is the most common AOP for its mild reaction conditions, convenient generation of HO• and satisfying degradation of contaminants without toxic by-products [6]. However, in homogeneous Fenton reactions, the difficulty in separating or recovering/recycling Fe catalysts from water and the narrow usable pH range are main obstacles for practical use [7]. Therefore, heterogeneous Fenton reaction is a promising process because of its long-term activity, easy recovery/recycling of catalysts from water, and no iron hydroxide precipitation [8, 9]. In general, there are three types of heterogeneous Fenton systems, that is, natural iron minerals [10], iron-oxides (Fe@Fe_2O_3 [11], Fe_3O_4 [12] etc.) and Fe-immobilized porous materials (such as clay [13, 14], mesoporous silica [15, 16], zeolite [17, 18] and carbon [19, 20] etc.).

In Fenton reaction, the reaction rate constant between Fe^{2+} and H_2O_2 (K = 70 $M^{-1}\cdot s^{-1}$) [21] is remarkably larger than that between Fe^{3+} and H_2O_2 (K = 0.0001 ~ 0.01 $M^{-1}\cdot s^{-1}$) [22]. Therefore, the proportion of Fe^{2+} in Fenton catalysts is a key point in determining their catalytic activity [23, 24]. Fortunately, amorphous FeO_x usually contains large proportions of Fe^{2+} due to its low crystallization and large amount of defects. Furthermore, amorphous FeO_x generally has higher surface area, more active sites than iron oxide crystals [25] caused by its higher surface-bulk ratio and more "dangling bonds" [26]. All these are believed to endow amorphous FeO_x with high catalytic activity in Fenton reaction.

Ferric oxide-immobilized porous catalysts have been extensively used in Fenton reaction because of their large pore volume and high surface area which are believed to improve their catalytic activity. Nevertheless, the wet impregnation method commonly used to incorporate Fe-based catalysts into porous matrix usually leads to aggregation of iron oxide particles and blockage of pore channels [27], thus resulting in generation of large amount of inaccessible active sites and consequently low catalytic activity in Fenton reaction.

Herein, a simple physical-vapor-infiltration (PVI) method has been developed to incorporate extraordinarily large amount of amorphous FeO_x without blocking the pore channels of mesoporous silica SBA-15. As heterogeneous Fenton catalysts, the obtained FeO_x/SBA-15 showed high catalytic activity in degrading Acid orange 7 (AO7).

Experimental

PVI incorporation of amorphous FeO_x into mesoporous silica

SBA-15. Mesoporous silica SBA-15 was synthesized according to a procedure published elsewhere [28]. 1 g ferrocene and 0.2 g calcined SBA-15 were together put into a tightly sealed jar. Then the PVI process was carried out at 110 ºC for different duration time. The obtained yellow brown powders were finally calcined at 400, 450, 500, 550 and 600 ºC in air, respectively. The obtained composites were denoted as FeO_x/SBA-nh-T, where nh and T represent the PVI duration time and calcination temperature, respectively.

Characterizations. Powder X-ray diffraction (XRD) patterns were recorded on a Rigaku D/MAX-2250 V D/Max 2200PC diffractometer using Cu-Kalpha radiation (40 kV and 40 mA). The scanning rate was 4 º·min^{-1} and 0.6 º·min^{-1} for the wide angle and small angle XRD measurements, respectively. Field Emission Transmission Electron Microscopy (FETEM) analysis was conducted with a JEOL 200CX electron microscope operated at 200 kV. Energy dispersive X-ray (EDX) spectrum was obtained from an attached Oxford Link ISIS energy-dispersive spectrometer fixed on a JEM-2010 electron microscope operated at 200 kV. Scanning transmission electron microscopic (STEM) were obtained on a JEOL-2010F electron microscope operated at 200 kV. Nitrogen adsorption/desorption isotherms at 77 K were measured on a Micromeritics TriStar 3000 instrument. All samples were outgassed at 150 ºC for 12 h under flowing N_2 before the measurement. The specific surface areas were calculated by the Brunauer–Emmet–Teller (BET) methods. X-ray photoelectron spectroscopy (XPS) signals were collected on VG Micro MKII instrument using monochromatic Mg Kalpha X-ray at 1253.6 eV operated at 120 W. All the element binding energies were referenced to the C (1s) line situated at 284.6 eV. Fourier Transform Infrared (FTIR) spectra were obtained in the range of 1000-2000 cm^{-1} with a Nicolet iS10 FTIR spectrometer of a 4 cm^{-1} resolution with powders dispersed in KBr. UV-vis absorption spectra were conducted using a UV-3101PC instrument manufactured by Shimadzu Corporation. The Fe content and the leaching of Fe concentration of catalysts was evaluated by measuring the Fe concentration in the supernatant after Fenton reaction with ICP-OES (Vista AX). Total organic carbon (TOC) was measured using a Shimadzu TOC-Vcpn analyzer.

Adsorption performance and catalytic activity of FeO_x/SBA-15 in Fenton reaction. Acid orange 7 (AO7) was used as a probe dye to evaluate the catalytic activity of FeO_x/SBA-15. The AO7 concentrations were identified by the UV-vis spectrophotometer at 484 nm. All adsorption tests and degradation tests of AO7 by FeO_x/SBA-15 suspension were carried out in dark. Typically, 25 mL 100 mg·L^{-1} AO7 solution was magnetically stirred at ambient temperature and the desired pH values were adjusted using HCl solution or NaOH solution. Then 15 mg FeO_x/SBA-17-450 was added. For the adsorption kinetics studies, concentrations of AO7 at different time were measured on UV-vis spectrophotometer. The adsorption isotherms were carried out at the same conditions with different initial concentrations of AO7 between 50 and 500 mg·L^{-1}. For Fenton reaction, 15 mg FeO_x/SBA-15 was added into the AO7 solution of 100 mg·L^{-1} and the mixture was stirred for 2 h in dark to reach the adsorption equilibrium. The heterogeneous Fenton reaction was initiated by the addition of an appropriate amount of H_2O_2 (30 wt%). 3.0 mL reaction suspension was taken out by injection syringe and filtered through a 0.22 μm nylon membrane. The AO7 concentrations in filtrates were analyzed by a UV-vis spectrophotometer. The degradation efficiency (%) of dye was calculated by the following equation:

$$\text{Degradation efficiency} = (C_0 - C) \times 100\% / C_0 \quad (1)$$

where C_0 and C stand for the initial and instant concentrations at different reaction time of AO7, respectively.

Results and discussion

Characterizations of FeO_x/SBA-15

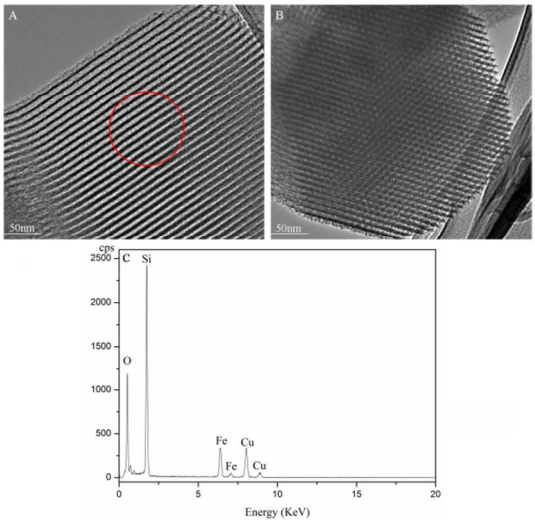

Fig. 1 TEM images (A, B) of the sample FeO_x/SBA-17h-450 and the EDX spectrum (C) collected from the circled area shown in (A).

Fig. 1A and B show the TEM images of the sample FeO_x/SBA-17h-450 taken with electron beams being perpendicular and parallel to the mesopore channels of SBA-15, respectively. It can be seen that the FeO_x/SBA-17h-450 has highly ordered hexahedral mesoporous structure as same as SBA-15 [28]. The Fe content in FeO_x/SBA-17h-450 obtained by EDX spectrum (Fig. 1C) is as high as 26.64 wt%. Surprisingly, there are no observable particle aggregations both inside and outside of its pore channels, demonstrating the thoroughly uniform dispersion of FeO_x species in the pore channels of the substrate, which ensures their high accessibility for reactants during catalytic reaction. This can be ascribed to the fact that it was sublimated metal-organic precursor, which can easily penetrate deep into the pore channels of SBA-15, that the PVI strategy used, to get rid of particle aggregates resulting from solvent surface tension [29].

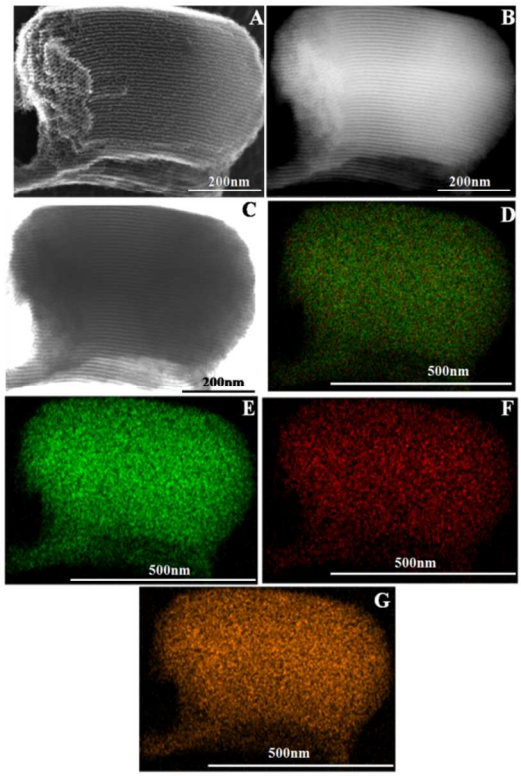

Fig. 2 STEM images of the FeO_x/SBA-17h-450 and the corresponding element mappings of the sample: D (Si, Fe, O), (E) Si, (F) Fe, (G) O.

Fig. 2 (A, B, C) show secondary electron (SE) image, high-angle annular dark-field (HAADF) image, bright filed (BF) image of FeO_x/SBA-17h-450, respectively. No FeO_x particles or aggregates could be observed on the outside surface of catalyst, even when the FeO_x content is as high as 26.64wt%, which is further identified by the HAADF image since no bright spots can be observed. BF image further shows the unblocked channel of the obtained composites. Element mapping by STEM confirmed that ferric species were highly dispersed in SBA-15 matrix (Fig. 2F).

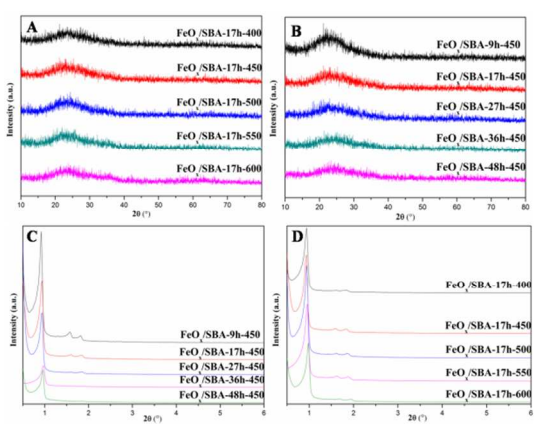

Fig. 3 Wide angle (A, B) and Small angle (C, D) XRD patterns of FeO_x/SBA-15 samples.

Fig. 3 shows the wide (A, B) and small angle XRD (C, D) patterns of FeO_x/SBA-15 samples. As can be seen in Fig. 3A and B, there is only one highly broadened peak corresponding to amorphous SiO_2 of SBA-15. No peaks of ferric oxide can be identified, indicating that FeO_x is amorphous and well-confined in the mesopore channels, as also verified by TEM (Fig. 1A, B). Three peaks indexed as (100), (110) and (200) reflections of the P6mm hexagonal mesoporous structure of SBA-15, respectively, can be found in their small angle XRD patterns as shown in Fig. 3(C, D), demonstrating their highly ordered mesoporous structure have well-maintained after FeO_x loading.

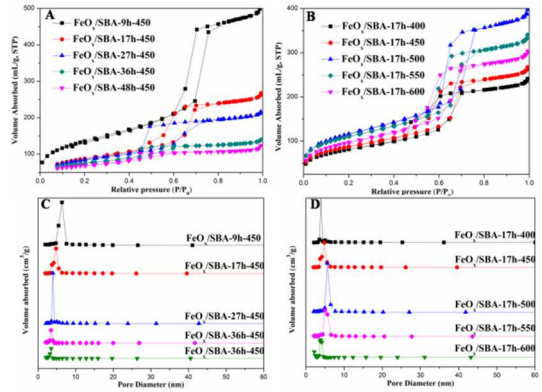

Fig. 4 The N_2 adsorption–desorption isotherms (A, B) and corresponding pore size distributions (C, D) of FeO_x/SBA-15 samples.

Their pore structures were further characterized by N_2 adsorption–desorption isotherms. As shown in Fig. 4, all the samples show a type IV isotherm with a H1 hysteresis loop at $P/P_0 > 0.5$ associated with capillary condensation, and steep jumps in the N_2 adsorption volume, indicating their mesoporous structures and narrow pore size distributions. Their specific surface area, pore size and pore volume data are all listed in Table. S1. For longer PVI durations, larger amount of FeO_x can be loaded, which results in decreased surface areas, pore volumes/diameters. Even so, their pore channels still remain open and accessible, as also confirmed by TEM, indicating the ferric oxide has been most probably deposited onto the inner mesopore channel surface of SBA-15 as a thin coating.

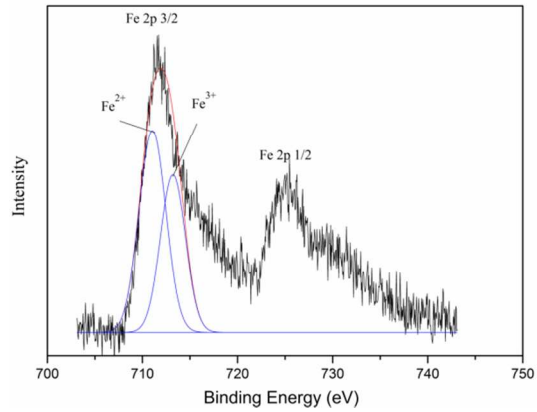

Fig. 5 XPS spectra of Fe 2p of FeO_x/SBA-17h-450.

The surface chemical composition and chemical state of FeO_x/SBA-15 were analyzed by XPS. Fig. 5 shows the Fe 2p spectrum of FeO_x/SBA-17h-450, in which two characteristic peaks at about 711 eV and 713 eV corresponding to Fe^{2+} and Fe^{3+} [30], respectively, can be found. The proportion of Fe^{2+} was

calculated to be 58% relative to 42% of Fe^{3+}, which could be beneficial for the high degradation efficiency of AO7 as mentioned above. The high proportion of Fe^{2+} can be due to the low crystallization and large amount of defects of amorphous FeO_x. Fig. S1 shows the XPS spectra of Fe 2p of FeO_x/SBA-17h-T. And Table S2 shows the proportion of Fe^{2+} and Fe^{3+} of FeO_x/SBA-17h-T, from which we can see all the materials contain high proportion of Fe^{2+}.

Adsorption performance and Fenton catalysis activity of FeO_x/SBA-15.

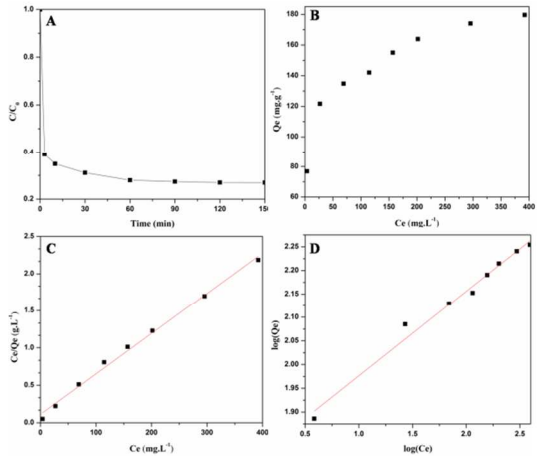

Fig. 6 (A) The adsorption kinetic curves of AO7 on FeO_x/SBA-17h-450, (B) The adsorption isotherm of AO7 on FeO_x/SBA-17h-450, (C) Langmuir and (D) Freundlich adsorption isotherms of AO7 on FeO_x/SBA-17h-450.

The adsorption of AO7 on FeO_x/SBA-15 was investigated prior to the Fenton reaction. Fig. 6A shows the adsorption kinetics curve of AO7 on FeO_x/SBA-17-450. The AO7 concentration decreased rather quickly at the initial stage and afterwards decreased further but slowly. Adsorption equilibrium was achieved in 2 h and about 73% of the dye AO7 was absorbed. The isoelectric point of FeO_x/SBA-17h-450 was indentified to be at pH 2.5-2.7 and AO7 is an anionic dye with $-SO_3$. Therefore, it was electrostatic favorable adsorption for AO7 on FeO_x/SBA-15, which has been further verified by the fact that the equilibrium concentration of AO7 decreased with the decrease of pH values, as shown in Fig. S6C. The adsorption isotherm of AO7 on FeO_x/SBA-17h-450 at pH=3 has been shown in Fig. 6B and simulated by Langmuir and Freundlich equations:

Langmuir isotherm: $C_e/Q_e = 1/(Q_mK_L) + C_e/Q_m$

Freundlich isotherm: $Log(Q_e) = Log(K_F) + (1/n)Log(C_e)$

where Q_e ($mg{\cdot}g^{-1}$) is the equilibrium adsorption capacity for AO7, C_e ($mg{\cdot}L^{-1}$) is the equilibrium concentration of AO7; Q_m ($mg{\cdot}g^{-1}$) and K_L ($L{\cdot}g^{-1}$) are Langmuir constants related to adsorption capacity and energy of adsorption, respectively. K_F ($mg{\cdot}g^{-1}$) and 1/n are the Freundlich constants, indicating the capacity and intensity of adsorption, respectively.

AO7 uptake by FeO_x/SBA-17h-450 was better fitted to Langmuir model than Freundlich model with $r^2 = 0.99355$ and the fitted Langmuir equations is $C_e/Q_e = 0.11235 + 0.00541C_e$. The excellent correlations assumed that all surface sites on the adsorbents have the same affinity for the adsorbate, the single adsorbate binds to a single site on the adsorbent to form a monolayer adsorption and no interactions between the adsorbates.

The degradation of AO7 by FeO_x/SBA-15 was further investigated. Fig. S2 shows UV–vis spectra changes of AO7 solution during Fenton reaction. It's obvious that the specific peak of azo bonds of AO7 at 484 nm disappeared in 10 min, indicating the complete degradation of AO7.

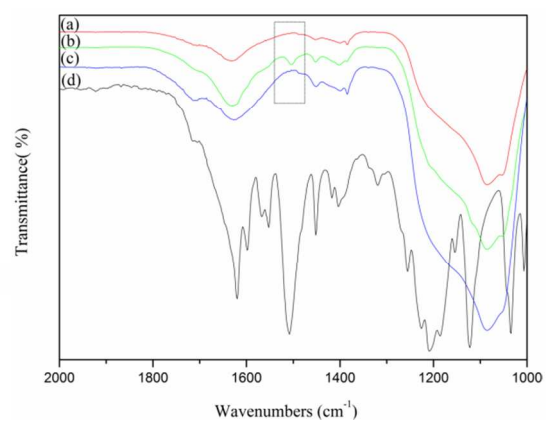

Fig. 7 FTIR spectra of FeO_x/SBA-17h-450 (a), AO7-adsorbed FeO_x/SBA-17h-450 before Fenton reaction (b), AO7-adsorbed FeO_x/SBA-17h-450 after Fenton reaction (c), and AO7 (d).

The FTIR spectra (Fig. 7) were used to characterize the structural change of AO7 molecules absorbed on FeO_x/SBA-15 before and after degradation. The intense adsorption of AO7 at 1514 cm^{-1} can be attributed to the vibrati ons of –N=N– bond or aromatic ring sensitive to the interaction with the azo bond, or to the N–H bending vibration mode (N–H) of the hydrazone form of the azo dye [31]. While most of the peaks of AO7 adsorbed on FeO_x/SBA-15 were overlapped by the strong and broad band of FeO_x/SBA-15 in the range of 1000–1200 cm^{-1}, the specific vibration peak at 1514 cm^{-1} of AO7 at FeO_x/SBA-15 can still be identified. The disappearance of the pea k at 1514 cm^{-1} after Fenton reaction indicates the degradation of AO7 absorbed on FeO_x/SBA-15. All these indicate AO7, both absorbed on the catalyst and in the solution, has been degraded completely. The mineralization degree of AO7 was examined by TOC analysis of the solution, as shown in Fig. S3. The TOC removal of the AO7 solution in 10 min reached above 60%, implying FeO_x/SBA-15 can induce an extremely fast mineralization of AO7 by Fenton reaction. As a comparative, commercial Fe_3O_4 was used to degrade AO7 at the same conditions. Fig. S4 clearly showed that it can only degrade 27% in 10 min and 66% in 2 h, demonstrating the huge advantage of FeO_x/SBA-15 in heterogeneous Fenton reaction.

Effect of PVI duration on AO7 degradation

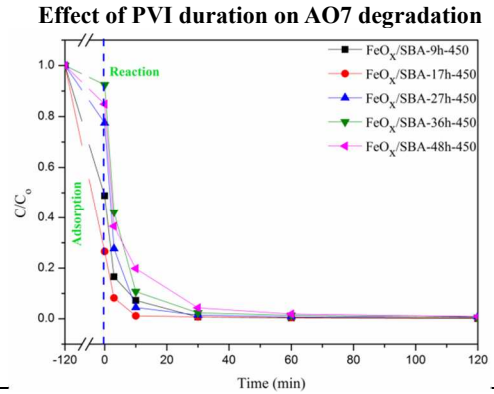

Fig. 8 Influence of PVI duration on the catalytic activity of FeO_x/SBA-15 (calcination temperature = 450 ºC, [FeO_x/SBA-15] = 0.6 g·L^{-1}, [H_2O_2] = 10 mM, pH_0 = 3, C_0 = 100 mg·L^{-1}).

The prolonged PVI duration, can lead to the increased FeO_x loading amount in SBA-15 and the decreased surface area, pore size/volume of FeO_x/SBA-15, which will noticeably affect their catalytic activity in Fenton reaction. Fig. 8 gives the concentration variations of AO7 during the adsorption to equilibrium and the following degradation reaction initiated by H_2O_2 addition. FeO_x/SBA-17h-450 demonstrates the best adsorption capacity and catalytic degradation activity for AO7. FeO_x/SBA-9h-450 has larger BET surface area, but has lower adsorption capacity and catalytic activity than FeO_x/SBA-17h-450 due to its smaller amount of active sites. FeO_x/SBA-15 obtained at PVI durations above 17 h have higher FeO_x contents as shown in Table S1, but show decreases in the adsorption capacity and degradation efficiency of AO7, which can be attributed to decreases of their BET surface areas and pore sizes/volumes.

Nevertheless, for all FeO_x/SBA-nh-450 samples, regardless of FeO_x amounts loaded, one hour is mostly enough to completely degrade AO7. Sample FeO_x/SBA-17h-450 can completely eliminate the dye in as short as 10 min by Fenton reaction.

Effect of calcination temperature on AO7 degradation

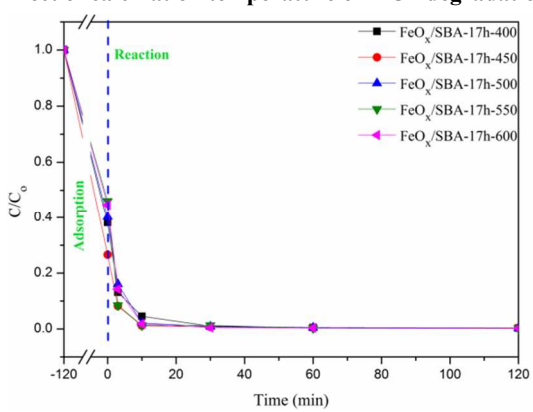

Fig. 9 Influence of calcination temperature on the catalytic activity of FeO_x/SBA-15 (PVI duration time = 17 h, [FeO_x/SBA-15] = 0.6 g·L^{-1}, [H_2O_2] = 10 mM, pH_0 = 3, C_0 = 100 mg·L^{-1}).

Firstly, the adsorption capacity of the catalysts obtained at different calcination temperatures can be related not only to their BET surface areas but also to the carbon residue after calcination in the catalysts (as shown in Fig. S5). As the decomposition temperature of ferrocece is 400 ºC, the higher the calcination temperature was, the less the content of carbon in the catalyst is. FeO_x/SBA-17h-450 shows the best adsorption capacity, which should be attributed to the best combination of carbon content and the BET surface area. As reported in literatures, the catalytic activity of heterogeneous catalysts in Fenton reaction is dependent on their calcination temperature and amorphous oxides obtained at low calcination temperature are inclined to show high catalytic activity [32, 33]. Here, the degradation of AO7 by the heterogeneous Fenton reaction on FeO_x/SBA-15 obtained at different calcination temperatures was investigated. Limited effects of calcination temperature of FeO_x/SBA-15 on catalytic degradation activity can be found as shown in Fig. 9. This could be attributed to the confinement effect of the mesopore channels of SBA-15 (Fig. 3 and 4), which lead to the compactness rather than particle growth of FeO_x coating on the mesopore surface during calcination at high temperature.

Effect of Fenton reaction conditions on AO7 degradation. Varied catalyst amounts from 0 to 1 g·L^{-1} were used to investigate the effect of FeO_x/SBA-17h-450 dosage on AO7 degradation efficiency. As can be seen in Fig. S6A, negligible degradation of AO7 can be found without FeO_x/SBA-17h-450, indicating that H_2O_2 itself cannot generate HO• to initiate Fenton reaction. With the increase of catalyst dosage, AO7 degradation was accelerated by the increased HO• concentration. The optimal concentration of FeO_x/SBA-17h-450 is 0.6 g·L^{-1}, above which no significant enhancement in degradation efficiency can be obtained.

It is well established that H_2O_2 shows significant effect on the degradation of dyes involving Fenton reaction. Consequently, effect of H_2O_2 dosage on the degradation of AO7 was investigated. As shown in Fig. S6B, no degradation of AO7 can be observed without H_2O_2. The degradation efficiency was improved by the increasing concentration of H_2O_2 until it reached 15 mM. At over-low initial concentration of H_2O_2, only limited amount of HO• can be generated, which is too little to initiate quick dye degradation. However, the excessive H_2O_2 with concentration above 15 mM, according to the following equations:

$$H_2O_2 + HO\bullet \rightarrow HO_2\bullet + H_2O \quad \text{eq. (1)}$$

$$HO_2\bullet \rightarrow O_2\bullet^- + H^+ \quad \text{eq. (2)}$$

the scavenging effect of HO• will happen and produce less active HO_2• and superoxide anion O_2•$^-$ [34] and thus retard the Fenton reaction.

Surface charge generally shows great influence on the catalytic activity of Fenton catalysts [35] since the adsorption of the dye molecules on catalyst surface and their catalytic degradation by HO• are synergetic [36]. As shown in Fig. S6C, with the decrease of pH from 9 to 2, both the adsorption performance and degradation efficiency can be promoted. Under alkaline conditions, only a small amount of dye could be adsorbed and no significant degradation of the dye was observed. Comparatively, in strong acid environment, the catalyst showed higher adsorption capacity and degradation efficiency for AO7 because the catalyst surface was nearly-positively (The isoelectric point was pH = 2.5-2.7) charged and easily adsorbed negatively-charged AO7 molecules by electrostatic interaction. Furthermore, it has been reported that an acid environment, in which the maximum amount of HO• can be produced, are usually optimum for Fenton reaction [37]. However, at pH = 2, little increase of degradation efficiency can be observed since excessive Cl^- can serve as HO• scavenger [38]. It is worth noting that the degradation efficiency could reach 89% in 120 min at pH = 5, indicating the catalyst are still effective in weak acid environment.

Stability and recycling performance of the heterogeneous Fenton catalyst FeO_x/SBA-15

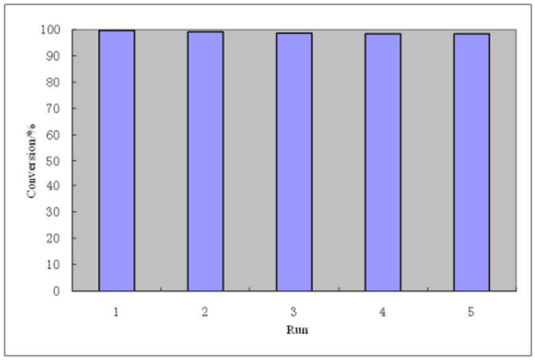

Fig. 10 Recycling performance of the FeO_x/SBA-17h-450 catalyst in degrading AO7 ([FeO_x/SBA-15] = 0.6 g·L^{-1}, [H_2O_2] = 15 mM, pH_0 = 3, C_0 = 100 mg·L^{-1}).

In order to investigate the stability of the FeO_x/SBA-15 catalysts, the dissolved iron concentration in the aqueous solution were tested by ICP-OES. At pH = 3, the concentration of total iron ions dissolved in the solution in 30 min after the adding of H_2O_2 was 5.77 ppm. To clarify whether it was a homogeneous reaction or heterogeneous reaction, the supernatant collected by centrifuging to remove FeO_x/SBA-15 solid during Fenton reaction was used to degrade AO7 and a degradation efficiency of as low as 20% was obtained after 2 h. The catalysts were recovered by centrifuging and dried in oven at 60 ºC for 12 h and then reused for AO7 degradation. The degradation efficiency of AO7 on FeO_x/SBA-15 only showed a slight decrease from 98% to 95% after five recycles (Fig. 10). These facts confirm it is a heterogeneous Fenton reaction that dominates the dye degradation on FeO_x/SBA-15.

Fenton catalytic mechanism on FeO_x/SBA-15. Scavenging study was used to further identify the responsibility of HO• in this Fenton reaction. The degradation of AO7 was significantly inhibited and decreased from 99% to 77% by adding 2-propanol (molar ratio 2-propanol/AO7 = 400/1), which is a typical HO• scavenger, to the reaction solution (Fig. S7), Taking account into the 73% removal of AO7 by adsorption on FeO_x/SBA-15, the degradation of AO7 by Fenton catalyst was negligible in the presence of 2-propanol, that is, without HO•.

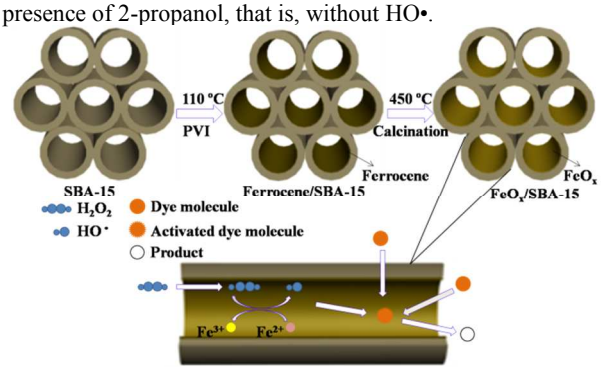

Fig. 11 Schematic diagram of the FeO_x/SBA-15 synthesis and application as heterogeneous Fenton catalyst for efficient degradation of AO7.

A synergistic catalytic effect, which is featured with the successional functions of the catalyst components in activating dye molecules by adsorption on the pore surface of the catalyst, and generating the active HO• species by Fe^{2+}/Fe^{3+} cycling after the dye adsorption, was assumed as illustrated in Fig. 11 [36]. The processes of the dye activation and HO• generation are independent of each other. Therefore, theoretically, the two processes can be regarded as in parallel. Nevertheless, in the practical operation of the Fenton reactions, dye molecules were first adsorbed and activated on the pore surface of FeO_x/SBA-15, then the HO• generated by the reaction between Fe^{n+} and later-added H_2O_2 oxidizes the activated dye molecules to small molecules or CO_2 and H_2O.

Conclusions

A simple physical vapor infiltration process has been developed to load extraordinarily large amount of ferric oxide into ordered mesoporous silica SBA-15. The FeO_x, which is demonstrated to be deposited as a thin coating on the mesopore channel surface of SBA-15, are amorphous and enriched with Fe^{2+} ions (58%, relative to 42% Fe^{3+}). The high dispersion of a large amount of Fe^{2+}-rich FeO_x species and the well-opened mesoporous structure of the composite catalysts are believed to the main contributors to the high performance in AO7 dye degradation (~ 99% AO7 degradation in 10 min at pH = 3, [H_2O_2] = 15 mM, and [FeO_x/SBA-15 catalyst] = 0.6 g·L^{-1}). The Fenton reaction is proposed to progress by a synergetic effect featured with the successional/parallel functions of catalyst components in dye adsorption-activation on the pore surface of the catalyst and the generation of active HO• species by Fe^{2+}/Fe^{3+} cycling, which are responsible for the high catalytic activity in the dye degradation. The catalyst also showed good stability with negligible decrease of degradation efficiency after 5 recycles. These mesoporous FeO_x/SBA-15 composites obtained by the low-cost convenient PVI approach are promising candidates as high-efficiency heterogeneous Fenton catalysts for water treatment.

Acknowledgments

The authors gratefully acknowledge financial support from National Key Basic Research Program of China, 2013CB933200, National Natural Science Foundation of China (Grant No. 21177137), Science and Technology Commission of Shanghai Municipality (11JC1413400).

Notes and references

[a]*State Key Laboratory of High Performance Ceramics and Superfine Microstructure, Shanghai Institute of Ceramics, Chinese Academy of Sciences, 1295 Dingxi Road, Shanghai 200050, PR China. Fax: +86 21 52413122; Tel: +86 21 52412712; E-mail: jlshi@mail.sic.ac.cn*

[b]*Faculty of Material Science and Chemistry, China University of Geosciences, Wuhan 430074, PR China*

† Electronic Supplementary Information (ESI) available: [Pore structure parameters; UV–vis spectra changes of AO7solution with reaction time; TOC; Degradation efficiency of AO7; Influence of catalyst dosage, H_2O_2 dosage, initial pH value on the catalytic activity; Effect of HO• scavenger 2-propanol on the catalytic activity]. See DOI: DOI: 10.1039/b000000x/

(1) Correia, V. M.; Stephenson, T.; Judd, S. J. *Environmental Technology* **1994**, *15*, 917.

(2) Aleksić, M.; Kušić, H.; Koprivanac, N.; Leszczynska, D.; Božić, A. L. *Desalination* **2010**, *257*, 22.

(3) Martínez-Huitle, C. A.; Brillas, E. *Applied Catalysis B: Environmental* **2009**, *87*, 105.

(4) Roberto Andreozzi , V. C., Amedeo Insola , Raffaele Marotta *Catalysis Today* **1999**, *53*, 51.

(5) Neyens, E.; Baeyens, J. *Journal of Hazardous Materials* **2003**, *98*, 33.

(6) Walling, C. *Accounts Chem. Res.* **1975**, *8*, 125.
(7) Hartmann, M.; Kullmann, S.; Keller, H. *J. Mater. Chem.* **2010**, *20*, 9002.
(8) Soon, A. N.; Hameed, B. H. *Desalination* **2011**, *269*, 1.
(9) Kasiri, M. B.; Aleboyeh, H.; Aleboyeh, A. *Applied Catalysis B: Environmental* **2008**, *84*, 9.
(10) Matta, R.; Hanna, K.; Chiron, S. *The Science of the total environment* **2007**, *385*, 242.
(11) Zhihui Ai, L. L., Jinpo Li,Lizhi Zhang, Jianrong Qiu,and Minghu Wu *The Journal of Chemical Physics C* **2007**, *111*, 4087.
(12) Niu, H.; Zhang, D.; Zhang, S.; Zhang, X.; Meng, Z.; Cai, Y. *J Hazard Mater* **2011**, *190*, 559.
(13) Sze Nga Sum, O.; Feng, J.; Hu, X.; Lock Yue, P. *Chemical Engineering Science* **2004**, *59*, 5269.
(14) Ramirez, J. H.; Costa, C. A.; Madeira, L. M.; Mata, G.; Vicente, M. A.; Rojas-Cervantes, M. L.; López-Peinado, A. J.; Martín-Aranda, R. M. *Applied Catalysis B: Environmental* **2007**, *71*, 44.
(15) Martínez, F.; Calleja, G.; Melero, J. A.; Molina, R. *Applied Catalysis B: Environmental* **2005**, *60*, 181.
(16) Martínez, F.; Calleja, G.; Melero, J. A.; Molina, R. *Applied Catalysis B: Environmental* **2007**, *70*, 452.
(17) Chen, F.; Li, Y.; Cai, W.; Zhang, J. *J Hazard Mater* **2010**, *177*, 743.
(18) Zhou, X.; Cui, X.; Chen, H.; Zhu, Y.; Song, Y.; Shi, J. *Dalton Trans* **2013**, *42*, 890.
(19) Mesquita, I.; Matos, L. C.; Duarte, F.; Maldonado-Hodar, F. J.; Mendes, A.; Madeira, L. M. *J Hazard Mater* **2012**, *237-238*, 30.
(20) Nguyen, T. D.; Phan, N. H.; Do, M. H.; Ngo, K. T. *J Hazard Mater* **2011**, *185*, 653.
(21) Tyson Rigg, W. T., Joseph Weiss *The Journal of Chemical Physics* **1954**, *22*, 575.
(22) Cheves Walling, A. G. *J. Am. Chem. Soc.* **1973**, *95*, 2987.
(23) Rusevova, K.; Kopinke, F. D.; Georgi, A. *J Hazard Mater* **2012**, *241-242*, 433.
(24) Hanna, K.; Kone, T.; Medjahdi, G. *Catal. Commun.* **2008**, *9*, 955.
(25) Libor Machala, R. Z., and Aharon Gedanken *J. Phys. Chem. B* **2007**, *111*, 4003.
(26) D. N. Srivastava, N. P., A. Gedanken,, and I. Felner *J. Phys. Chem. B* **2002**, *106*, 1878.
(27) Liu, T.; You, H.; Chen, Q. *Journal of Hazardous Materials* **2009**, *162*, 860.
(28) Dongyuan Zhao, Q. H., Jianglin Feng,Bradley F. Chmelka,and Galen D. Stucky, *JournaloftheAmericanChemicalSociety* **1998**, *120*, 6024.
(29) Kyung-Bok Lee, S.-M. L., Jinwoo Cheon *Advanced Materials* **2001**, *13*, 517.
(30) Ramirez, J. H.; Maldonado-Hódar, F. J.; Pérez-Cadenas, A. F.; Moreno-Castilla, C.; Costa, C. A.; Madeira, L. M. *Applied Catalysis B: Environmental* **2007**, *75*, 312.
(31) Gao, Z.; Cui, F.; Zeng, S.; Guo, L.; Shi, J. *Microporous and Mesoporous Materials* **2010**, *132*, 188.
(32) Deng, J.; Jiang, J.; Zhang, Y.; Lin, X.; Du, C.; Xiong, Y. *Applied Catalysis B: Environmental* **2008**, *84*, 468.
(33) Miao, Z.; Tao, S.; Wang, Y.; Yu, Y.; Meng, C.; An, Y. *Microporous and Mesoporous Materials* **2013**, *176*, 178.
(34) Bigda, R. J. *Chemical Engineering Progress* **1995**, *91*, 62.
(35) Gumy, D.; Morais, C.; Bowen, P.; Pulgarin, C.; Giraldo, S.; Hajdu, R.; Kiwi, J. *Applied Catalysis B: Environmental* **2006**, *63*, 76.
(36) Shi, J. *Chem Rev* **2013**, *113*, 2139.
(37) SCOTT M. A R N O L D , W. J. H. I. C. K. E. Y., R O B I N F . H A R R I S *Environmental Science & Technology* **1995**, *29*, 2083.
(38) J . K I W I , A. L. O. P. E. Z., V . N A D T O C H E N K O *Environ. Sci. Technol* **2000**, *34*, 2162.

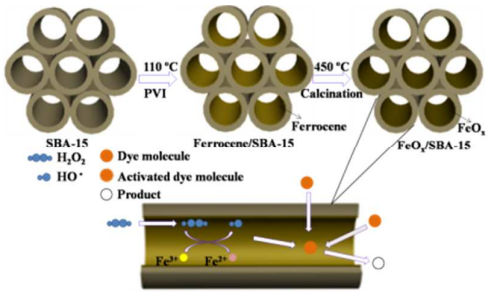

High dispersion of large amount of Fe^{2+}-rich FeO_x and unblocked pore channels of catalysts obtained by physical-vapor-infiltration facilitate Fenton reaction.